

# Modeling of Compression Curves of Flexible Polyurethane Foam with Variable Density, Chemical Formulations and Strain Rates

M.F. Alzoubi<sup>1,\*</sup>, S. Al-Hallaj<sup>1</sup>, M. Abu-Ayyad<sup>2</sup>

<sup>1</sup>Director of Research & Development, All Cell Technologies LLC, Chicago, IL USA

<sup>2</sup>ME Department, Penn State Harrisburg, Middletown, PA USA

Received 9 November 2013; accepted 24 January 2014

## ABSTRACT

Flexible Polyurethane (PU) foam samples with different densities and chemical formulations were tested in quasi-static stress-strain compression tests. The compression tests were performed using the Lloyd LR5K Plus instrument at fixed compression strain rate of  $0.033 \text{ s}^{-1}$  and samples were compressed up to 70% compression strains. All foam samples were tested in the foam rise direction and their compression test stress results were modeled using a constitutive Polymeric or Phenomenological Foam Model (PFM). In this research, a new constitutive PFM model that consists of mechanical systems such as dashpots and springs was formulated to be used for different strain rate experiments. The experimental compression test results for different strain rates were compared to the PFM model results for all foam samples. Both modeling and experimental results showed pretty good agreement. From curve fitting of the experimental tests with the PFM model; different mechanical materials' coefficients such as elastic and viscous parameters were computed. These mechanical parameters are indeed important characteristics for viscoelastic materials. This model can be used for constant and variable strain rates and for characterizing biomechanical material applications such as bone tissues, muscle tissues and other cellular materials.

© 2014 IAU, Arak Branch. All rights reserved.

**Keywords:** Polyurethane foam; Phenomenological foam model; Maxwell arm; Compression curves; Viscoelastic parameters; Characteristics length time; Biomechanics; Maxwell model; Kelvin-Voigt model

## 1 INTRODUCTION

**P**OLYMERIC polyurethane foams have important usage in several industrial applications in energy absorptions and comfort bedding applications [1, 2]. Foam can be used also in cushions of car seats, pillows, beddings, packaging, acoustic absorption and upholstery. Comfort, vibration isolation and crashworthiness structures are one of the primary means used in most modern automobile seats, furniture and bedding [3]. Foams usually are nonlinear viscoelastic materials and are interesting structures that possess unique mechanical and thermal properties in nature which attracted engineers, scientists and researchers to examine it. Recent studies showed that there is strong evidence that some of the mechanical properties such as stiffness and viscoelastic characteristics of cellular materials have similar mechanical response and thermal behavior as those in tissues and muscles in human body. This attracted many researchers, medical doctors and scientists to investigate and learn about these materials

\* Corresponding author. Tel.: +1 773 922 1155.

E-mail address: malzoubi@allcelltech.com (M.F. Alzoubi).

as well. The static and dynamic behavior of these cellular materials is also sensitive to compression levels, strain rates, temperature, amplitude and frequency of excitation.

The PFM model for solid foam materials for an individual layers was presented by Goga et al. [4], such materials when they exposed to compression loading, they can be mechanically modeled using the PFM model. This model describes the uniaxial compression behavior of foam materials but it is restricted for constant strain rates. Another recent decent work was done by Jeong et al. [5], which he proposed a new constitutive model that highlights the strain rates dependency. Jeong model was derived by Nagy et al [6]. In this paper, the new constitutive model presented has the strain rates dependency as Jeong et al. However, it was derived by a combination of Maxwell and Kelvin-Voigt models which include mechanical systems such as springs and dashpots. These dashpots and springs are designed to build up the three distinct regions of polyurethane compression model. Such models have significant characteristics for viscoelastic materials and biomechanical applications such as those in cancellous bone models which were introduced by [7]. Mechanical properties of cellular materials are heavily depended on foam density and other parameters such as investigated by [8, 9]. Several models were also developed to describe the compressive deformation and mechanical properties for polyurethanes cellular materials such as those in [10-13]. It was shown in this research that the experimental stress-strain compression curves of the flexible polyurethane foam materials for different densities can be predicted using the PFM model but with strain rates dependency. Also in this study, the PFM model was extended to be used for any variable strain rates. This model is also valid for any material that possesses viscoelastic characteristics such as tissues and muscles.

Another recent unique work in modeling foam cell structures was conducted by [14]. In this work, a micromechanics model for three dimensional open-cell foams using a tetrakaidecahedral unit cell model and Castigliano's second theorem was developed. Each tetrakaidecahedral unit cell as shown in Figure 1 has 36 struts and was treated as uniform slender beams undergoing linearly elastic deformations. They also incorporated the struts with different cross sectional shapes such as circular, square, equilateral triangle and plateau border. Out of these findings, two closed-form formulas for determining the effective Young's modulus and Poisson's ratio of open-cell foams were provided. The new formulas explicitly show that the foam elastic properties depend on the relative foam density, the shape and size of the strut cross section, the Young modulus and the Poisson's ratio of the strut material.

In a similar work, Li, Gao et al. [15] developed their micromechanical modeling by using the tetrakaidecahedral unit cell foam as shown in Fig. 1 along with the matrix method for spatial frames instead of the Castigliano's second theorem. In this model, the formulas for determining the effective Young's moduli, Poisson's ratios and shear moduli of open cell foams are derived using the composite homogenization theory. This theory confirms that foam elastic properties depend on the relative foam density, the shape and size of the strut cross-section, the Young's modulus and the Poisson's ratio of the strut material which is on agreement with [14] above.

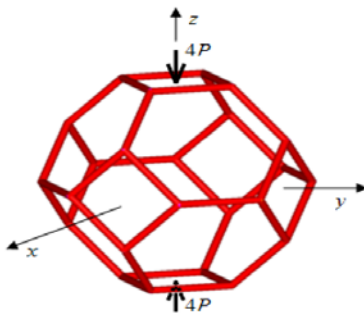


**Fig. 1**  
A tetrakaidecahedral unit model of an open foam cell.

In biomechanics' applications, Zhang et al. [16] validated the strain rate dependency on finite element analysis (FEA) model of the Rodent Traumatic Brain Injury. Also, Saha et al. [8] studied and measured peak stress within the elastic range and the energy absorption up to 15% strain and they concluded that these measurements are highly depending on foam density. Furthermore, Saha et al. [8] investigated peak stresses and energy absorption for open foam cells at 15% strains. In this unique research; all experiments were compressed up to 70% strains and peak stresses were measured.

Therefore, the focus of this research was first on deriving the mathematical polymeric foam model using a combination of Maxwell and Kelvin-Voigt models and carries this model for any variable strain rates. The second focus was on curve fitting the stress-strain experimental compression curves of the different density foam materials and different chemical formulations with the PFM mathematical model. From least square curve fitting procedure;

several damping and elastic coefficients of the Maxwell and Kelvin mechanical dashpot and spring systems can be extracted. Such coefficient numbers are very important to characterize, design and determine the viscous and the elastic behaviors of cellular materials. Changing these numbers and/or changing the Maxwell and Kelvin mechanical systems connection criteria shall affect the overall product design of these foam materials and can play a strong role in the overall performance of these foams when they are utilized in different applications.

## 2 FOAM STRUCTURE

Foam such as solid flexible polyurethane is cellular solids whose microstructure consists of an interconnected network of struts (open-cells) or plates (closed-cells) as shown in Fig.2. The voids which bordered by them thus create cells. These cells are usually filled by gas or liquid or just open cells. Natural materials, such as wood, cork and cancellous bone and man-made materials such as metal honeycombs, polymers and metal foams, are well-known examples of cellular solids.

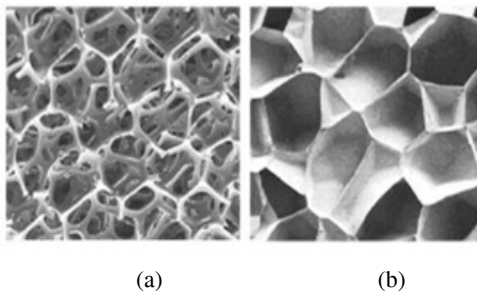


**Fig. 2**  
Examples of cellular foam; a) open-cell polyurethane foam, b) closed-cell polyurethane foam.

All foam samples of the stress-strain tests were compressed up to 70% strain. Historically; three main distinct regions are found for compression stress-strain curves of these flexible polyurethane foams as shown in Fig.3. These three regions exhibits an initial linear elastic region where strain energy is stored in reversible bending of the struts; a plateau region where struts begin to impinge upon each other and finally densification region where the foam at this stage becomes a solid material for such the cells start impinging each other causing a sudden increase in internal compression stiffness of the cellular network. During this final stage, the foam essentially becomes a solid composed of the solid material from which it is made of.

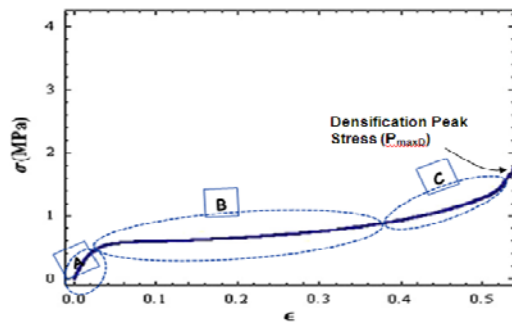


**Fig. 3**  
Stress-strain curve for PU foam sample under compression testing. A: linear elastic region, B: plateau region & C: densification region.

The density of foam is one among the most important mechanical properties of cellular materials. Several researches have done tremendous work to investigate the effect of the foam density on the foam stiffness, viscous behavior and energy absorption applications. Previous work was done by Gibson, et al. [9] and Alzoubi, et al. [10] where they described the effect of foam density on the mechanical properties for open and closed cells for cellular solids. For instance Gibson & Ashby, 1982 described density ratios as a function of the moduli of elasticity and plateau stress to the yield strength ratios of open cells for linear elastic region as follows:

$$E^*/E_s = C_1(\rho^*/\rho_s)^2 \quad (1)$$

For plateau region plastic foam:

$$\sigma_{pl}^* / \sigma_y = C_2 (\rho^* / \rho_s)^{3/2} \quad (2)$$

where  $E^*$  is Young's modulus of foam,  $E_s$  is the Young's modulus of cell wall material,  $\rho^*$  and  $\rho_s$  is density of foam and cell wall material of which the foam is made of, respectively, and  $C_1$  and  $C_2$  are constants and they can be determined by testing several foam samples with different densities. Likewise,  $\sigma_y$  is the yield strength of the cell wall material and  $\sigma_{pl}^*$  is the plateau stress

### 3 MECHANICAL PROPERTIES OF FOAM

It is worthwhile mentioning here that one of the major reasons causes differences in foam density when making foam is the amount of water that gets added during the foam rising process. Another reason of changing the foam density can be established by using a special catalyst or cross-linker agents or any other agents that be added to the foam recipe that results in certain criterion or thermal and mechanical properties. Researchers and scientists should be aware that in order to investigate the effect of density of the foam on the mechanical and the thermal properties; the foam samples should have the same chemical formulations, otherwise their comparisons won't be legitimate.

**Table 1**

Foam samples densities

Property	Group 2		Group 1			
	HR	Latex	PU55	PU85	PU100	PU110
Density $\rho$ (kg/m <sup>3</sup> )	40	85	55	85	100	110
Density of solid foam, $\rho_s$ (kg/m <sup>3</sup> )	–	–	1200	1200	1200	1200
Relative Density $\rho_s / \rho$	–	–	0.046	0.071	0.083	0.092

Table 1. shows all foam sample densities and their solid made densities. These two groups of foam materials were tested. The first group has four PU foam samples and they were labeled as PU55, PU85, PU100 and PU110. The symbol PU is an indication of polyurethane foam material and the associated number is an indication of the foam or polyurethane density measured in Kg/m<sup>3</sup>. These four samples were assumed to have the same chemical formulations but with different densities. Polyurethane (PU) polymers are traditionally and most commonly formed by reacting a di- or poly isocyanate with a polyol. The second group has two other foam samples and they were labeled as HR which represents high resilient low density material and the Latex to represent latex materials. HR material is another form of polyurethane foam compound but with different additives and water quantity amounts. Latex material is the stable dispersion of polymer micro particles in an aqueous medium. Latexes may be natural or synthetic and it can be made synthetically by polymerizing a monomer such as styrene that has been emulsified with surfactants. Both of Latex and HR foam samples have totally different chemical formulations and different density when compared to group No.1. Usually HR and latex foam samples are used in high resilience applications, whereas the four PU foam samples used for high impact absorption and also for comfort applications such as seating and beddings. One of the other focuses of this research was to investigate the effect of density of the four samples on elastic and viscous characteristics of foam materials. Moreover; the research was extended further to investigate the effect of the chemical formulations of the two foam groups on viscoelastic parameters of Kelvin and Maxwell models. All tests were conducted at constant temperatures of 25°C and they were compressed at a fixed strain rate of 0.033 s<sup>-1</sup> to 70% strain. All foam samples were tested in the direction of foam rise (thickness).

#### 4 POLYMERIC MAHEMATICAL MODEL (PFM) FOR FOAM MATERIALS WITH SINGLE LAYER

Goga et al. [4] described a new phenomenological model for foam materials. The purpose of this model was to come up with a new simpler model that has few parameters and can be an easy tool to be used for predicting the behavior of the compression of the stress-strain curve for polyurethane foam. Since polyurethane foam is a nonlinear viscoelastic material; Goga et al. replaced this material with mechanical components such as springs and dashpots. Springs represent an elastic component with restorative forces and dashpots represent a viscous component with damping forces. Connecting a spring and a dashpot in series yields the Maxwell model as shown in Fig. 4(a). This is also called the Maxwell arm. While connecting a spring and dashpot in parallel yields the Kelvin Voight model as in Fig. 4(b). Designing different mechanical combinations of these basic models give the opportunity for engineers to modeling viscoelastic materials with different mechanical output behaviors.

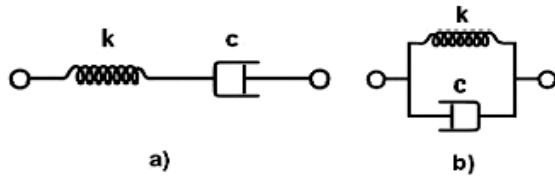


**Fig. 4**  
a) Maxwell arm model, b) Kelvin-Voight model.

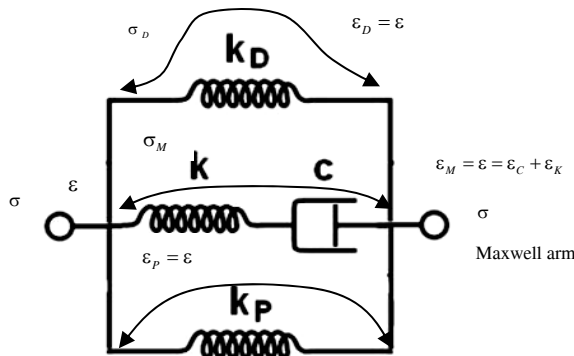


**Fig. 5**  
The Polymeric phenomenological foam model.

The PFM model that Goga generated is shown in Fig. 5. This model is a combination of a Maxwell arm model which located in the middle of Fig. 5. From the sides of the model a couple of springs were connected in parallel to the Maxwell arm. The first spring system from the lower part of the PFM model in Fig. 5 has a spring stiffness of  $K_P$  which simulates the linear spring stiffness in the plateau region which is also shown in Fig. 6. The middle portion of the model represents the Maxwell arm in Fig. 6. The Maxwell arm of the PFM model is a combination of the spring stiffness  $k$  and the damping viscosity  $c$  of the dashpot. The last portion from the top part of Fig. 5 represents the second spring system  $K_D$  which covers the nonlinear spring stiffness system in the densification region of Fig.6. The compression stress-strain response of the Maxwell arm along with the linear and the nonlinear spring coefficients are shown in details in Fig. 5.

Eq. (3) below represents the total stress of the PFM model from Fig.5 and it contains three components of stresses; the first stress term  $\sigma(\epsilon, \dot{\epsilon})_M$  represents the Maxwell arm stress, the second term  $\sigma(\epsilon)_P$  represents the plateau stress and the last term  $\sigma(\epsilon)_D$  represents the densification stress component.

$$\sigma(\epsilon, \dot{\epsilon}) = \sigma(\epsilon, \dot{\epsilon})_M + \sigma(\epsilon)_P + \sigma(\epsilon)_D \quad (3)$$

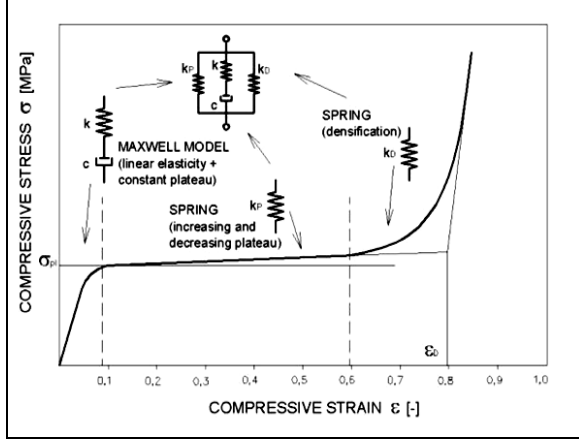


**Fig. 6**  
Stress-strain of the new foam model.

where  $\sigma(\varepsilon, \dot{\varepsilon})_M$  is the stress generated in the elastic and the viscous regions (i.e. the Maxwell arm),  $\sigma(\varepsilon)_p$  is the stress generated in the plateau region and  $\sigma(\varepsilon)_D$  is the stress generated in the densification region. In order for modeling the system shown in Fig.5 which represents the stress strain compression curves, the following physical relations must realize;

For the series components:

$$\sigma_M = \sigma_K = \sigma_C \quad (4)$$

where  $\sigma_M$  is the stress generated in the Maxwell arm,  $\sigma_K$  is the stress generated in the spring element of the Maxwell arm and finally  $\sigma_C$  is the stress generated in the dashpot element of the Maxwell arm.

$$\varepsilon_M = \varepsilon_K = \varepsilon_C \quad (5)$$

where  $\varepsilon_M$  is the total strain generated in the Maxwell arm,  $\varepsilon_K$  is the strain generated in the spring element and  $\varepsilon_C$  is the strain generated in the dashpot of the Maxwell arm.

For the parallel components:

$$\sigma = \sigma_M + \sigma_p + \sigma_D \quad (6)$$

where  $\sigma_p$  and  $\sigma_D$  represent the stress generated in the plateau and the densification regions, respectively.

$$\varepsilon_M = \varepsilon_K + \varepsilon_C = \varepsilon_D = \varepsilon_p = \varepsilon \quad (7)$$

where  $\varepsilon_p$  is the strain generated in the spring element of the Plateau region and  $\varepsilon_D$  is the strain generated in the spring element of the densification region.

Defining the stress for the individual stress components of Eq. (6) yields;  $\sigma_K = K\varepsilon_K$ ,  $k$  is the stiffness of the spring element in the Maxwell arm.

$\sigma_C = C\dot{\varepsilon}_C$ , where  $c$  is the damping coefficient of the dashpot and  $\dot{\varepsilon}_C$  is the strain rate of the dashpot.

$\sigma_p = K_p\varepsilon_p$ , where  $K_p$  is the stiffness of the spring in densification region.

$$\sigma_D = \varepsilon_D\gamma(1 - e^{-\varepsilon})^n \quad (8)$$

where  $\gamma$  is the densification coefficient and  $n$  is the polynomial exponent of the nonlinear spring element in densification region.

For Maxwell model the stress  $\sigma(\varepsilon, \dot{\varepsilon})_M$ , total strain  $\varepsilon_M$  from Eq. (5) and their rate strain rates of change as a function of time are governed by equation:

$$\dot{\varepsilon}_M = \frac{\dot{\sigma}_M}{K} + \frac{\sigma_M}{C} \quad (9)$$

If we multiply Eq. (9) by  $Kc$ , we get

$$Kc\dot{\varepsilon}_M = C\dot{\sigma}_M + K\sigma_M \quad (10)$$

Eq. (10) represents a nonlinear first order differential equation and it can be solved by the integral method technique.

Multiply Eq.(10) by the integral factor  $e^{\int \frac{K}{C} dt}$ , Eq. (10) becomes

$$e^{\int \frac{K}{C} dt} . Kc\dot{\varepsilon}_M = e^{\int \frac{K}{C} dt} . C\dot{\sigma}_M + e^{\int \frac{K}{C} dt} . K\sigma_M \quad (11)$$

Thus  $e^{\int \frac{K}{C} dt} = e^{\frac{K}{C}t}$ , therefore Eq.(11) becomes;

$$e^{\frac{K}{C}t} Kc\dot{\varepsilon}_M = e^{\frac{K}{C}t} . C\dot{\sigma}_M + e^{\frac{K}{C}t} . K\sigma_M \quad (12)$$

$$e^{\frac{K}{C}t} Kc\dot{\varepsilon}_M = \frac{d}{dt} (e^{\frac{K}{C}t} . C\sigma_M) \quad (13)$$

Multiply both sides of Eq. (13) by  $dt$  and integrate both sides, Eq. (13) yields;

$A_1 + \int e^{\frac{K}{C}t} Kc\dot{\varepsilon}_M dt = e^{\frac{K}{C}t} . C\sigma_M$ , where  $A_1 = \text{constant}$ , simplify and rearrange, this equation can be written as:

$$\sigma_M = \frac{A_2 + \int e^{\frac{K}{C}t} Kc\dot{\varepsilon}_M dt}{e^{\frac{K}{C}t} . C} \quad (14)$$

Therefore,

$$\sigma_M = \frac{1}{C} e^{-\frac{K}{C}t} (A_1 + Kc \int e^{\frac{K}{C}t} \dot{\varepsilon}_M dt) \quad (15)$$

with the help of integral by parts terminology;  $\int q'p dt = qp - \int qp' dt$

Therefore,

$$\int \dot{\varepsilon}_M e^{\frac{K}{C}t} dt = \varepsilon_M e^{\frac{K}{C}t} - \int \varepsilon_M \frac{K}{C} e^{\frac{K}{C}t} dt \quad (16)$$

Therefore, Eq. (15) can be rewritten as;

$$\sigma_M = \frac{1}{C} e^{-\frac{K}{C}t} \left( A_1 + Kc \left\{ \varepsilon_M e^{\frac{K}{C}t} - \int \varepsilon_M \frac{K}{C} e^{\frac{K}{C}t} dt \right\} \right) \quad (17)$$

or

$$\sigma_M = \frac{A_1 e^{-\frac{K}{c}t}}{c} + K\varepsilon_M - \frac{e^{-\frac{K}{c}t}}{c} \int \varepsilon_M \frac{K}{c} e^{\frac{K}{c}t} dt \quad (18)$$

Eq. (18) shows the general compression stress equation of the foam Maxwell arm for any strain rate function. In this paper, all tests were conducted at constant strain rate, therefore if  $\dot{\varepsilon}_M = a_1$ , where  $a_1$  is a constant, then  $\varepsilon_M = a_1 t$ , therefore Eq. (15) can be written as;  $\sigma_M = \frac{1}{c} e^{-\frac{K}{c}t} (A_1 + Kc \int e^{\frac{K}{c}t} a_1 dt)$ , solving the integral part; this equation can be written as:

$$\sigma_M = \frac{1}{c} e^{-\frac{K}{c}t} (A_1 + Kca_1 e^{\frac{K}{c}t} \frac{c}{K}) = \frac{1}{c} e^{-\frac{K}{c}t} (A_1 + c^2 a_1 e^{\frac{K}{c}t}) \quad (19)$$

It depends on the strain rate function;  $A_1$  can be found by the boundary conditions accordingly, substitute  $t = 0$  at  $\sigma_M = 0$ , Eq.(19) becomes:

$A_1 + c^2 a_1 = 0, A_1 = -c^2 a_1$ ; substitute  $A_1$  in Eq. (19), Eq. (19) can be written as:

$$\sigma_M = \frac{1}{c} e^{-\frac{K}{c}t} (-c^2 a_1 + c^2 a_1 e^{\frac{K}{c}t}) = ca_1 e^{-\frac{K}{c}t} (-1 + e^{\frac{K}{c}t}) \quad (20)$$

$\dot{\varepsilon}_M = a_1$  then  $\varepsilon_M = a_1 t = \dot{\varepsilon}_M t$ ; and  $t = \frac{\varepsilon_M}{\dot{\varepsilon}_M}$ ; therefore Eq. (20) can be written as:

$$\sigma_M(\varepsilon, \dot{\varepsilon}_M) = c \dot{\varepsilon}_M e^{-\frac{K \varepsilon_M}{C \dot{\varepsilon}_M}} (-1 + e^{\frac{K \varepsilon_M}{C \dot{\varepsilon}_M}}) \quad (21)$$

Eq. (21) presents the general compression stress equation of the foam Maxwell arm for constant strain rates. Combine Eqs. (6), 8 and 21 results in the total stress equation stress of Fig. 5.

$$\sigma(\varepsilon, \dot{\varepsilon}) = e^{-\frac{K \varepsilon_M}{C \dot{\varepsilon}_M}} (-1 + e^{\frac{K \varepsilon_M}{C \dot{\varepsilon}_M}}) C \dot{\varepsilon}_M + \varepsilon_p K_p + \varepsilon_D \gamma (1 - e^\varepsilon)^n \quad (22)$$

Substitue  $\varepsilon_M = \varepsilon_D = \varepsilon_p = \varepsilon$ ; Eq. (22) becomes

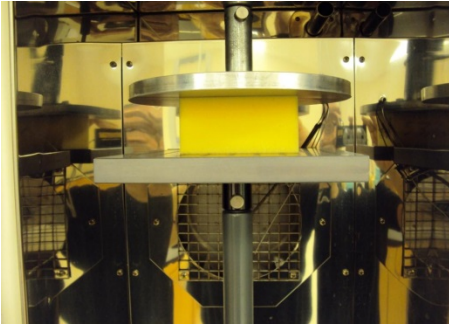
$$\sigma(\varepsilon, \dot{\varepsilon}) = e^{-\frac{K \varepsilon}{C \dot{\varepsilon}}} (-1 + e^{\frac{K \varepsilon}{C \dot{\varepsilon}}}) C \dot{\varepsilon} + \varepsilon K_p + \varepsilon \gamma (1 - e^\varepsilon)^n \quad (23)$$

Eq. (23) represents the overall general compression stress equation of the foam for three regions of the foam which includes the Maxwell arm region, the plateau and finally the densification regions.

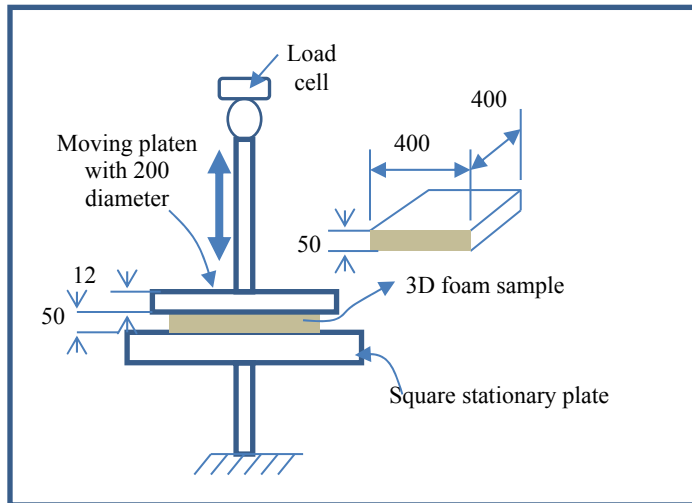
#### 4 TEST METHOD

Six foam samples labeled with HR, Latex, PU55, PU85, PU100 and PU110 were cut with dimensions of 400 mm x 400 mm x 50 mm for which all samples were tested in the 50 mm (foam rise) direction. Quasi-static compression tests with 20 cm diameter platen using the Lloyd LR5K Plus instrument as shown in Fig.7(a). was performed at constant strain rates of 0.033 s<sup>-1</sup>.

Fig.7(b). shows also a schematic diagram of the Lloyd instrument that was used for performing the compression tests. All experiments were conducted at constant temperatures of 25°C. The compression tests of the stress-strain curve tests were recorded as a function of time using a data acquisition program. Stresses at 5% and 70% strains were measured and recorded for all foam samples. Elastic moduli of elasticity of the polyurethane foam samples were calculated at stresses that were measured at 5% strain which represents the linear elastic portion of the compression stress-strain curve of the polyurethane.

**Fig. 7(a)**

Lloyd LR5K Plus instrument with an enclosure.

**Fig. 7(b)**

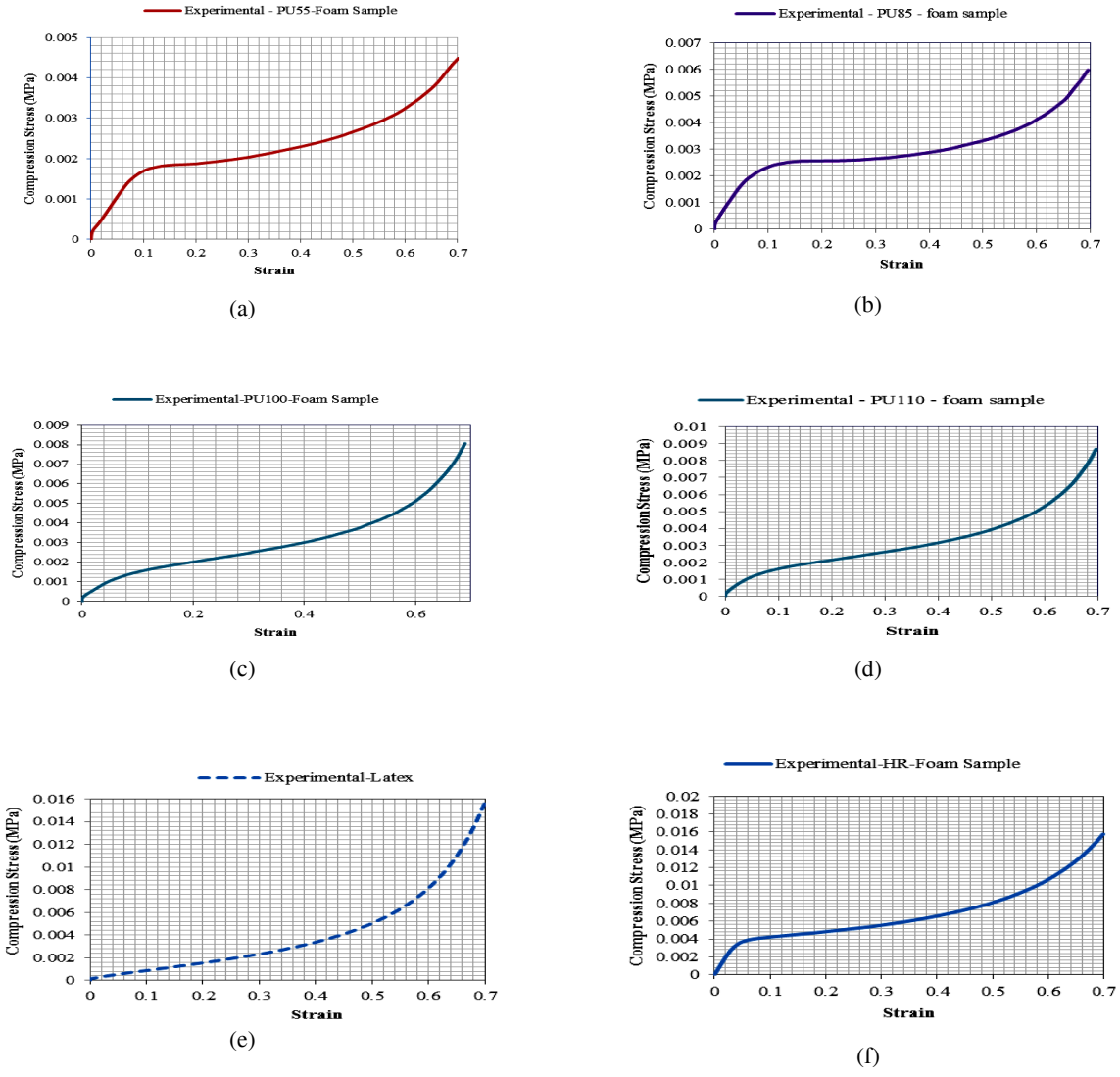
Schematic diagram of the Lloyd compression testing.

## 5 RESULTS AND DISCUSSION

### 5.1 Experimental compression tests layer of the foam samples

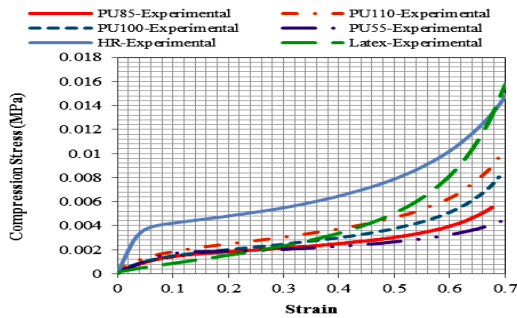
Uniaxial quasi-static compression tests were performed for all foam samples that were shown in Table 1. For these particular tests, a strain rate of  $0.033 \text{ s}^{-1}$  was kept constant. The quasi-static experimental stress-strain compression test curves of the six foam samples PU55, PU85, PU100, PU110, Latex and HR are shown in Figs .8(a), 8(b), 8(c), 8(d), 8(e) and 8(f ) respectively.

Fig.9 shows the experimental stress-strain of the compression responses for all foam samples were plotted on one graph. It is obvious that the experimental curve for HR material has the highest compression stresses among all other foam samples. Also, the figure shows that the Latex curve has less viscous characteristics than other foam samples. Usually samples with high viscoelastic characteristics show a plateau or a hump reflection point around 5-10% strains. This indicates that the Latex material has no distinct three regions as the case for other samples. This is indeed emphasizing that latex material has highly elastic and low viscous characteristics than any other foam samples. Table 2 shows stresses measured at 5% and 70% compression strains, and Young modulus calculated at 5% compression strains for all six foam samples. Young moduli were calculated by dividing stresses measured at 5% strain by 0.05 strains.



**Fig.8**

a)Quasi-static compression test response of PU55 foam sample. b)Quasi-static compression test response of PU85 foam sample. c)Quasi-static compression test response of PU100 foam sample. d) Quasi-static compression test response of PU110 foam sample. e)Quasi-static compression test response of Latex foam sample. f)Quasi-static compression test response of HR foam sample.



**Fig. 9**

Quasi-static compression test response of all foam samples.

**Table 2**  
Elastic stress outputs at 5% strains, 70% strains and Young Modulus.

Foam Sample	Stresses at 5% Strain; (KPa)	Young's Modulus ( $E^*$ ) calculated at 5% Strains; (KPa)	Max. Stresses measured at 70% Strain; (KPa)
HR	3.80	76.0	14.8
Latex	0.55	11.0	15.5
PU55	0.90	18.0	4.50
PU85	0.92	18.4	6.40
PU100	1.00	20.0	8.80
PU110	1.20	24.0	14.0

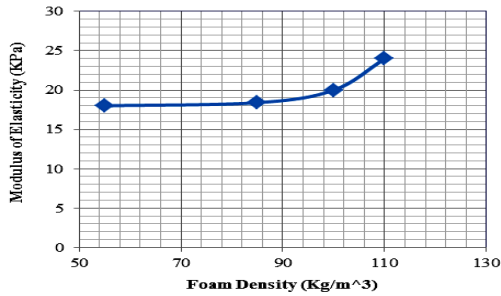


**Fig. 10**  
Modulus of elasticity versus foam density for PU55, PU85, PU100 & PU110 foam samples.

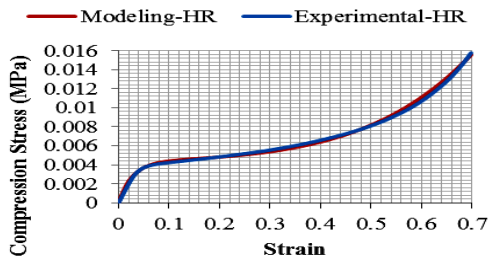


**Fig. 11**  
Quasi-static compression test response for experimental versus Phenomenological model of the HR foam sample.

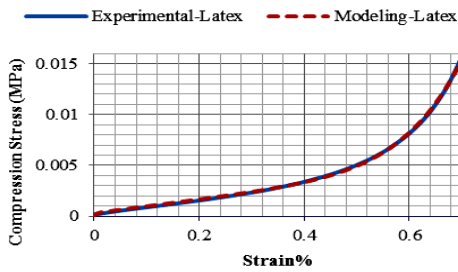


**Fig. 12**  
Quasi-static compression test response for experimental versus Phenomenological model of Latex foam sample.

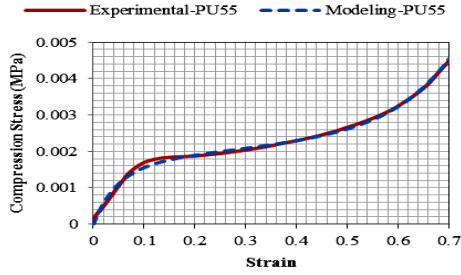


**Fig. 13**  
Quasi-static compression test response for experimental versus Phenomenological model PU55 foam sample.

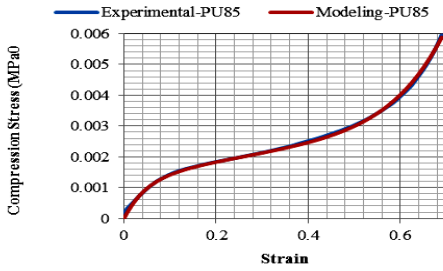


**Fig. 14**  
Quasi-static compression test response for experimental versus Phenomenological model of PU85 foam sample.

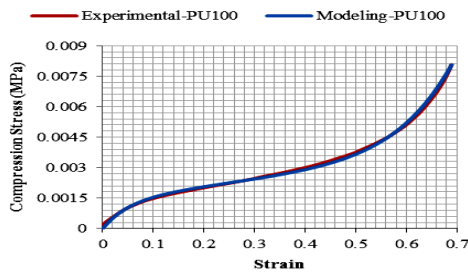


**Fig. 15**  
Quasi-static compression test response for experimental versus Phenomenological model of PU100 foam sample.

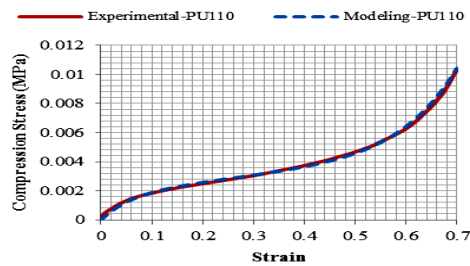


**Fig. 16**  
Quasi-static compression test response for experimental versus Phenomenological model of PU110 foam sample.

Table 2 also shows that HR and Latex foam samples were placed in separate rows than the other four foam samples. This is to indicate that these two samples have totally different chemical formulations and usages than other foam samples. When comparing the other foam samples among each other; it's obvious to notice that Young's moduli increases with foam density and this is shown in Fig.10. Also Fig.10 shows that the modulus of elasticity increases rapidly around foam samples with higher densities than those at lower density values.

Furthermore, Table 2 shows stresses measured at 5% and 70% which are both increased with density. It is worth noted that when investigate the effect of the chemical formulations of the six samples on the moduli and stresses at 5 and 70% strains, the Young modulus of HR is almost four times than other four samples, and indeed the maximum stresses also was the highest among all samples. Practically, these observations should be considered in designing beds, seats or any other comfort or energy absorption applications. It is also obvious that HR material has the highest modulus of elasticity while the Latex material has the lowest modulus of elasticity. Interestingly, it is found that even though Latex material has very low stiffness at small strains, it gets very stiff at higher compression strains.

### 5.2 Curve fittings of the experimental compression tests with PFM

All experimental compression tests of the six foam samples of Fig. 9 were curve fitted using the least square method of the Polymeric model of Eq. (23). The model curves were plotted against the experimental tests for each foam samples in Figs. 11-16.

It is clear from Figs. 11-16 that all experimental tests were on a good agreement with the curve fitting of the Polymeric foam models. Using the least square curve fitting method; the PFM model of Eq.(23) can be fitted into the experimental tests of the six foam samples, then different mechanical parameter outputs can be extracted such as those in Table 3.

**Table 3**

Model Parameter Outputs of the Different Foam Samples Based on the Polymeric Model of Eq. (23).

Material	$d\varepsilon/dt$ (1/sec)		Maxwell Arm Constants			Characteristic Time Length	Plateau Region	Densification Coeff.	n
	Strain Rate	$E^*$ , Mpa Modulus of Elasticity	Stress MPa Stress @ 70%	c (MPa .sec) Damping Coeff.	k (MPa) Spring Coeff.	T (sec) c/k	$k_p$ (MPa) Spring Coeff.	(MPa) $\gamma$	
HR	0.0333	0.0760	0.0148	0.1300	1.200	0.11	0.0018	0.0140	2
Latex	0.0333	0.011	0.015	0.009	0.100	0.09	0.0068	0.014	4
PU55	0.0333	0.0180	0.0044	0.0480	0.033	1.45	0.0016	0.00245	4
PU85	0.0333	0.0180	0.0064	0.0400	0.027	1.48	0.0026	0.0410	4
PU100	0.0333	0.0200	0.0088	0.0430	0.0270	1.59	0.0033	0.0065	4
PU110	0.0333	0.0240	0.0140	0.0530	0.0300	1.77	0.0042	0.0077	4

Table 3 shows the different elastic and viscous model parameter outputs of the different foam samples. Also, the ratio of the damping coefficient  $C$  to the spring coefficient  $K$  of the Maxwell arm for each foam was added to the table. This ratio is an important physical phenomenon in viscoelastic materials and it's called the characteristic time length of the foam. The characteristic time length is an indication of the amount of the viscous forces of the Maxwell arm to those of the elastic forces, consequently it has the time unit. The longer the characteristic time is an indication that foam is highly viscous and the time for stress relaxation recovery is too slow. The same principle applies for shorter characteristic length time, the shorter the characteristics time is an indication that foam is highly resilient or elastic and the time for stress recovery is fast. Therefore, in order to estimate the amount of viscous behavior for a foam or for viscoelastic materials; researchers, engineers and scientists should be looking closely into the ( $c/k = T$ ) ratio rather than the damping  $c$  itself.

It is obvious from looking at the characteristic time lengths of the different foam samples in Table 3. that the foam density of PU55, PU85, PU100 and PU110 foam samples is directly proportional to the characteristic time length  $T$  of the foam and their time lengths range from 1.45-1.77 seconds. This concludes that the higher the foam density has results in longer characteristic time. However; HR and latex foam samples have the shortest characteristic time lengths which is 0.11, 0.09 seconds respectively. This is because HR and latex possess high resilience material responses and low viscous characteristics which results in shortening the characteristic time  $T$ . Such conclusion is very important in industrial applications specially when constructing a composite material that is made of several foam layers such as those in viscoelastic bedding and energy absorbers which they are well known in industrial applications.

### 5.3 Effect of foam density on foam model parameters

In order to investigate the effect of foam density on the elastic and the viscous parameters for foam samples of PU55, PU85, PU100 and PU110 foam samples. Elastic coefficients of the Maxwell arm stiffness (i.e.  $k$ ), plateau stiffness (i.e.  $k_p$ ), and densification (i.e.  $k_D$ ) coefficients can be plotted against the density ratios of the foam samples as shown in Figs. 17, 18, 19 and 20 respectively. Solid density  $\rho_s$  of 1200 kg/m<sup>3</sup> was used here to calculate

relative density. Table 4 shows the relative foam density and their corresponding damping and elastic foam parameters.

**Table 4**  
Foam Density Ratios and Their Model Paramters

Material	$\rho^*/\rho_s$	c (MPa .sec)	k (MPa)	kp (MPa)	$\gamma$ (MPa)
PU55	0.0458	0.0480	0.033	0.0016	0.00245
PU85	0.0708	0.0400	0.027	0.0026	0.0410
PU100	0.0833	0.0430	0.0270	0.0033	0.0065
PU110	0.0917	0.0530	0.0300	0.0042	0.0077

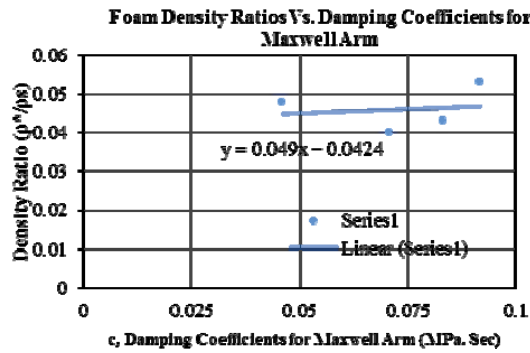


**Fig. 17**  
Foam density ratios Vs. damping coefficients for maxwell arms.

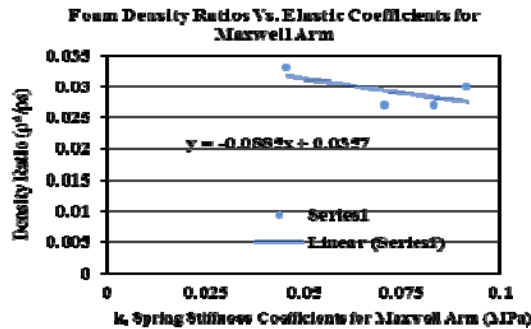


**Fig. 18**  
Foam density ratios vs. stiffness coffecinet for the maxwell arm springs.

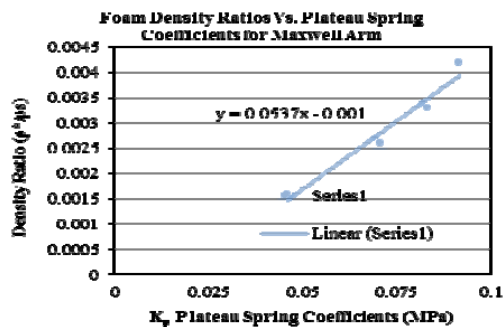


**Fig. 19**  
Foam density ratios Vs. plateau stiffness coffecinet.

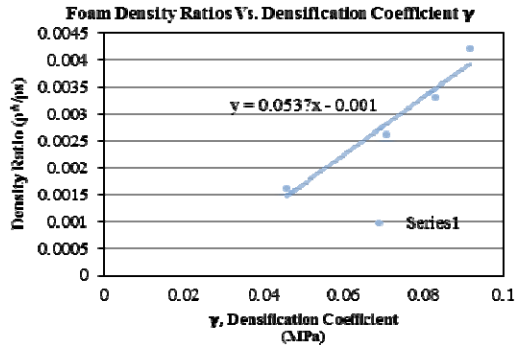


**Fig. 20**  
Foam density ratios Vs. densification coefficients.

Fig. 17 shows that there is a slight inverse correlation between the density ratios of the foam and their damping coefficients of the Maxwell arm. It is recommended to mention here that in order to come up with a solid correlation between density ratios and damping coefficients, further research should be extended to cover different ranges of low and high density beyond the scope of this research. Fig. 18 shows that increasing the foam density ratios results in decreasing the spring stiffness of the Maxwell arm. Figs. 19 and 20 show that increasing the density ratios of the foam causes the plateau spring stiffness and the densification coefficient to be increased.

## 6 CONCLUSIONS

It is clear from the discussion of previous results that the following conclusions can be extracted:

1. The Polymeric foam modeling equation is correlated perfectly to the experimental compression stress-strain curve of the Polyurethane Foam Model.
2. Viscoelastic materials such as flexible Polyurethane foams can be modeled with the polymeric foam equation using combinations of Maxwell Arm, plateau region and densification region.
3. For the Maxwell Arm, it is very imperative to characterize the material by looking closely at the characteristic length time ratio between the viscous forces of the dashpot to elastic forces of the spring.
4. The higher the characteristic time period is an indication that damping viscous forces of the Maxwell arm is overweighing the elastic forces.
5. The mathematical equation below of the compression stress-strain curve can be used to characterize viscoelastic materials for constant strain rates and constant temperatures.

$$\sigma(\varepsilon, \dot{\varepsilon}) = e^{-\frac{K \varepsilon_M}{C \dot{\varepsilon}_M}} \left( -1 + e^{\frac{K \varepsilon}{C \dot{\varepsilon}}} \right) C \dot{\varepsilon}_M + \varepsilon K_P + \varepsilon \gamma (1 - e^{\varepsilon})^n$$

6. The above equation can be used for modeling viscoelastic materials for constant strain rates, room temperatures and for compression stress applications; this equation can be extended to be used for biomechanical modeling applications such as muscles and tissues.
7. Controlling viscous and elastic parameter ratios is an essential process in designing and optimizing comfort and stiffness for bedding and seats and other viscoelastic industrial applications.
8. Polyurethane foams with density ranges 70-110 Kg/m<sup>3</sup> is a good material to be for high impact and comfort applications, whereas Latex and high resilient materials with lower density and different chemical formulations are good materials to be used for products demand bouncy applications such as bouncy mats.
9. This research can be extended for modeling multi layers of viscoelastic materials.

## ACKNOWLEDGMENTS

The authors would like to thank All Cell Technologies LLC, for their contribution to make this work a success.

## REFERENCES

- [1] Walter Timothy R., Richards Andrew W., Subhash G., 2008, A unified phenomenological model for tensile and compression response of polymeric foams, *Journal of Engineering Material Technology* **131**(1):011009-011015.
- [2] Jankowski M., Kotelko M., 2010, Dynamic compression tests of a polyurethane flexible foam as a step in modeling impact of the head to the vehicle seat head restraint, *FME Transactions* **38**:121-127.
- [3] Doutres O., Atalla N., Dong K., 2013, A semi-phenomenological model to predict the acoustic behavior of fully and partially reticulated polyurethane foams, *Journal of Applied Physics* **113**: 054901-054912.
- [4] Goga V., 2011, Testing and application of new phenomenological materials model for foam materials, *Computational Modeling and Advanced Simulations Series: Computational Methods in Applied Sciences* **24**:67-82.
- [5] Jeong K.Y., Cheon S.S., Munshi M. B., 2012, A constitutive model for polyurethane foam with strain rate sensitivity, *Journal of Mechanical Science and Technology* **26** (7): 2033-2038.
- [6] Nagy A., Ko W.L., Lindholm U. S., 1974, Mechanical behavior of foamed materials and dynamic compression, *Journal of Cellular Plastics* **10**:127-134.
- [7] Avramescu E.T., Călina M.L., Rusu L., 2009, New approaches to cancellous bone bio-modeling, *Romanian Journal of Morphology and Embryology* **50**(2):229-237.
- [8] Saha M.C., Mahfuz H., 2005, Effect of density, microstructure and strain rate on compression behavior of polymeric foams, *Journal of Material Science and Engineering A* **406**: 328-334.
- [9] Gibson L.J., Ashby M.F., 1988, *Cellular Solids: Structures and Properties*, Pergamon Press, Oxford, United Kingdom.
- [10] Alzoubi M.F., Tanbour E.Y., Al-Waked R., 2011, Compression and hysteresis curves of nonlinear polyurethane foams under different densities, strain rates and different environmental conditions, *Proceeding ASME* **9**: 101-109.
- [11] Rusch K.C., 1969, Load-compression behavior of flexible foams, *Journal of Applied Polymer Science* **13**:2297-2311.
- [12] Ashby M.F., 1983, The mechanical properties of cellular solids, *Metallurgical Transactions* **14**:1755-1769.
- [13] Gibson L.J., Ashby M.F., 1997, *Cellular Solids: Structures and Properties*, Cambridge University Press, United Kingdom.
- [14] Li K., Gao X.L., Roy A.K., 2003, Micromechanics model for three-dimensional open-cell foams using a tetrakaidecahedral unit cell and castigliano's second theorem, *Composites Science and Technology* **63**:1769-1781.
- [15] Li K., Gao X.L., Roy A.K., 2005, Micromechanics model for three-dimensional open-cell foams using the matrix method for spatial frames, *Composites Science and Technology* **36**: 249-262.
- [16] Zhang L., Gurao M., Yang K.H., King A.I., 2011, Material characterization and computer model simulation of low density polyurethane foam used in a rodent traumatic brain injury model, *Journal of Neuroscience Methods* **198**(1):93-98.